JOURNAL OF MATERIALS SCIENCE 16 (1981) 1103–1107

Solidification of metallic aerosol droplets from floating rafts: a test of the spiral growth mechanism for Cd and Zn

E. R. BUCKLE, P. TSAKIROPOULOS
Condensation Laboratory, Department of Metallurgy, The University, Sheffield, UK

The strain energy developed by surface stresses in a crystalline raft of basal orientation floating on a droplet of melt is calculated and compared to the strain energy of a screw dislocation situated on the raft axis. The suggestion that a dislocation is generated at a characteristic value of the raft/drop radius ratio is tested by making the comparison for arbitrary values of raft aspect ratio and Burgers vector. When $b = c$, the lattice parameter of the hexagonal crystal, the energies are equal at a combination of aspect ratio and radius ratio that fits experiment. The apparent height of the helical growth step greatly exceeds this value of b and remains to be explained, but the results confirm that a high growth rate anisotropy is required initially to produce the dislocation.

1. Introduction

The solidification of molten aerosol particles of Zn or Cd takes place by the nucleation and growth of floating basal rafts [1]. Growth occurs in two stages. The raft first spreads laterally over the liquid surface while remaining relatively thin. In the second stage there is rapid thickening. This involves the advance of the self-perpetuating step formed by a screw dislocation emergent at the solid–liquid interface. It was suggested [1] that the dislocation is the result of strain imposed by the surface forces, and the present paper is an attempt to verify this by calculating the raft dimensions at which the strain energy reaches the necessary level and comparing them to the experimental values.

2. The source of elastic strain energy

First the strain energy is evaluated in a flat, circular raft of radius a held on an unsupported liquid droplet of radius R (and of the same composition) by the surface forces acting at the edge and on the two basal faces. The system of drop plus raft is taken to be mechanically isolated and at constant temperature; the raft centre occupying a position fixed with respect to the drop centre. The raft is assumed to grow while held in the liquid surface without experiencing any forces, including thermal stresses, as the result of the exchange of internal or kinetic energy between the liquid and its surroundings.

If gravitation and buoyancy forces are also neglected, the forces on the floating raft may be depicted as in Fig. 1. The vertical load intensity q_v is an evenly distributed stress equal to the excess pressure. In the absence of a raft this would be given by $(2\gamma/R)$, where γ is the liquid surface tension. The basal surfaces of the raft introduce two new interfaces, and hydrostatic equilibrium requires the drop and the raft to deform so as to preserve a uniform pressure drop.

To avoid these complications and the related problem of the contact angle, it is assumed that $q_v = 2\gamma/R$ holds to sufficient accuracy and that the curvature of the liquid remains spherical up to the edge of the raft (Fig. 1c). The radial tension at the raft perimeter is represented by a load of intensity q_h, evenly distributed over the thickness $2c$. Resolving γ into vertical and horizontal components, γ_v and γ_h, as in Fig. 1c, we obtain for the equilibrium of vertical forces on the perimeter

$$2\pi a\gamma_v = \pi a^2 q_v, \quad (1)$$

whence

$$\gamma_v = aq_v/2 \quad (2)$$

and

0022–2461/81/041103–05$02.50/0

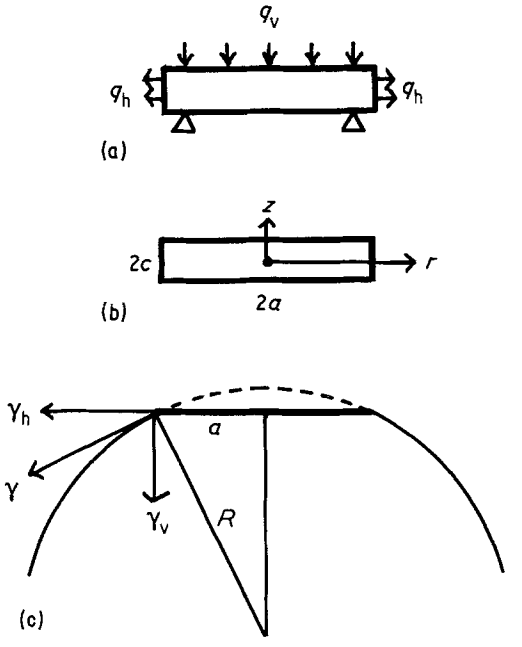

Figure 1(a) Loaded plate equivalent of floating raft, (b) raft dimensions and co-ordinate system (θ not shown) and (c) raft-drop geometry.

$$\gamma_h = \gamma_v(a/R)\,[1-(a/R)^2]^{\frac{1}{2}} = (q_vR/2)\,[1-(a/R)^2]^{\frac{1}{2}}. \quad (3)$$

The distributed tensile load, acting in the direction of γ_h, has intensity

$$q_h = \gamma_h/2c = (q_vR/4c)\,[1-(a/R)^2]^{\frac{1}{2}}. \quad (4)$$

Defining

$$y = a/R \quad (5)$$

then

$$q_h = (q_vR/4c)(1-y^2)^{\frac{1}{2}} \quad (6)$$

is obtained.

The quantity y, the raft/drop radius ratio, has been found experimentally to show a characteristic value, which will be denoted $y^* = a^*/R$, whenever the raft has grown to "maturity" and the dislocation mechanism of solidification has ensued. The value of y^* is 0.55 for Zn and 0.53 for Cd [2].

3. Elastic strain energy of a dislocation-free floating raft

The cylindrical polar co-ordinates r, θ, z and origin at the raft centre, where r is the length of the radius vector in the horizontal mid-plane and the polar axis z coincides with the raft axis (Fig. 1b) were chosen. Although for Zn and Cd the raft is isotropic only in the basal plane [3], it is supposed that along with the usual thin-plate simplifications [4, 5], the problem may be treated as one of the deformation of an isotropic plate freely supported under the perimeter and bearing a vertical load uniformly distributed over the surface on one side, and a radial load uniformly distributed over the thickness all round the perimeter (Fig. 1a). It is also assumed that a plane stress field results from the radial load that is independent of the vertical load [6], and that the total strain energy density V_0 may be obtained by separate evaluation and summation of the vertical and horizontal contributions V_{0v} and V_{0h}, respectively, i.e.

$$V_0 = V_{0v} + V_{0h}. \quad (7)$$

The total strain energy V for a raft of thickness $2c$ and radius a is then

$$V = \int_c^c \int_0^{2\pi} \int_0^a V_0 r\,dr\,d\theta\,dz. \quad (8)$$

The energy density for vertical loading reduces by the vanishing of the shear stress components $\tau_{r\theta}$ and $\tau_{\theta z}$ to

$$2V_{0v} = (\sigma_r + \sigma_\theta + \sigma_z)^2/E - (\sigma_\theta\sigma_z + \sigma_r\sigma_z + \sigma_r\sigma_\theta - \tau_{rz}^2)/G, \quad (9)$$

where the σ are the normal stresses and G is the modulus of rigidity. For horizontal loading (plane stress) σ_z and τ_{rz} also vanish to give

$$2V_{0h} = (\sigma_r + \sigma_\theta)^2/E - \sigma_r\sigma_\theta/G. \quad (10)$$

The following are the expressions for the stress components under vertical loading [4, 5]:

$$\sigma_r/q_v = (z/c)^3(2+\nu)/8 - 3(3+\nu)r^2z/32c^3 - 3(2+\nu)z/40c + 3(3+\nu)a^2z/32c^3; \quad (11)$$

$$\sigma_\theta/q_v = 3(3+\nu)a^2z/32c^3 - 3(1+3\nu)r^2z/32c^3 + (2+\nu)z/8c^3 - 3(2+\nu)z/40c; \quad (12)$$

$$\sigma_z/q_v = 3z/4c - z^3/4c^3 - 1/2; \quad (13)$$

$$\tau_{rz}/q_v = -3(c^2-z^2)r/8c^3. \quad (14)$$

Under horizontal loading, in view of the isotropy,

$$\sigma_r = \sigma_\theta = q_h \quad (15)$$

may be written.

TABLE I Data for calculation of V, [8–11]

Metal	T(K)*	E(GPa)	G(GPa)	γ(N m^{-1})†
Cd	573	30.4	11.7	0.59
Zn	673	54.9	22.0	0.77

*Solid at melting point – 20 K.
†Liquid at melting point.

The so-called distortional strain energy densities V'_0 are obtained by subtraction of the purely hydrostatic contributions from the complete expressions [7]

$$V'_{0v} = V_{0v} - (\sigma_r + \sigma_\theta + \sigma_z)^2(1-2\nu)/6E \quad \text{and} \tag{16}$$

$$V'_{0h} = V_{0h} - (\sigma_r + \sigma_\theta)^2(1-2\nu)/6E, \tag{17}$$

and the total distortional energy density $V'_0 = V'_{0v} + V'_{0h}$ integrates to yield the distortional energy

$$V' = \int_{-c}^{c}\int_0^{2\pi}\int_0^a V'_0 r\,dr\,d\theta\,dz. \tag{18}$$

Defining the raft aspect ratio by

$$x = a/c \tag{19}$$

and carrying out the integrations the following expression is obtained for the total strain energy

$$V/R = k_1x^3y^3 - k_2xy^3 + k_3y^3/x + k_4xy, \tag{20}$$

where y is the radius ratio defined in Equation 5. The values of the coefficients k obtained for Cd and Zn with the data of Table I are given in Table II.

An equation of similar form results for the distortional strain energy in the raft

$$V'/R = k'_1x^3y^3 - k'_2xy^3 + k'_3y^3/x + k'_4xy. \tag{21}$$

The values of the k' for the conditions of Table I are also given in Table II.

4. Energy of the axial screw dislocation

It was postulated in the previous paper [1] that as the raft expands elastic strain builds up to a level at which one or more screw dislocations with axes parallel to the raft axis are formed. It is found from the above expression for V_0 that strain concentrates in the vicinity of the raft axis, and is highest at the extremities ($z = \pm c$). The stress due to a screw dislocation is concentrated near the dislocation line, in this case also the raft axis. It is now assumed without consideration of the mechanism by which the stress field relaxes, that a sufficient criterion for spiral growth to commence is that the total strain energy rises to equal that of a single screw dislocation positioned on the axis and terminating on the basal faces.

The strain energy of an axial dislocation in a thin, elastically isotropic disc of infinite radius but finite thickness is given [12] by

$$V_d = (2cGb^2/4\pi)\ln(c/2.24r_i), \tag{22}$$

where r_i is the radius of a stress-free hole at the core and b is the modulus of the Burgers vector. The expression is probably sufficiently accurate for our purpose when restricted to discs with aspect ratios above about 5 [13]. It is convenient to re-write the expression for V_d in terms of x and y to give

$$V_d/R = (Gb^2/2\pi)(y/x)[\ln(y/x) + \ln(R/r_i) - 0.806]. \tag{23}$$

A value of 1 nm is taken for r_i [14], and since R varies typically from 1 to 50 μm for the spheres in our aerosols an average value of 8.86 for $\ln(R/r_i)$ is used. The unit cell height c or an integral multiple of it is approprite for b.

5. Results of calculations: raft thickness and helix step height

We now look for equality in the values of V/R and V_d/R for any size of drop, assuming first that the Burgers vector has the minimum value $b = c$ (data from [15]). Fig. 2 gives the results calculated for Cd at 573 K, at which temperature the molten metal is supercooled by 20 K.

The curves for V and V_d swing in opposite directions as parameter x is varied. For a thick raft (small x) there is no intersection at a meaningful raft radius ($y \leqslant 1$), so that there is never sufficient energy for the formation of a screw dislocation. Although the calculation of both V and V_d assumes the raft to be thin this result is to be

TABLE II Coefficients (pN) for the strain energy equations

Metal	T(K)	k_1	k'_1	k_2	k'_2	k_3	k'_3	k_4	k'_4
Cd	573	2.95	1.93	5.25	3.25	53.88	46.70	12.60	7.73
Zn	673	3.08	1.94	13.26	10.88	49.33	41.00	12.79	7.24

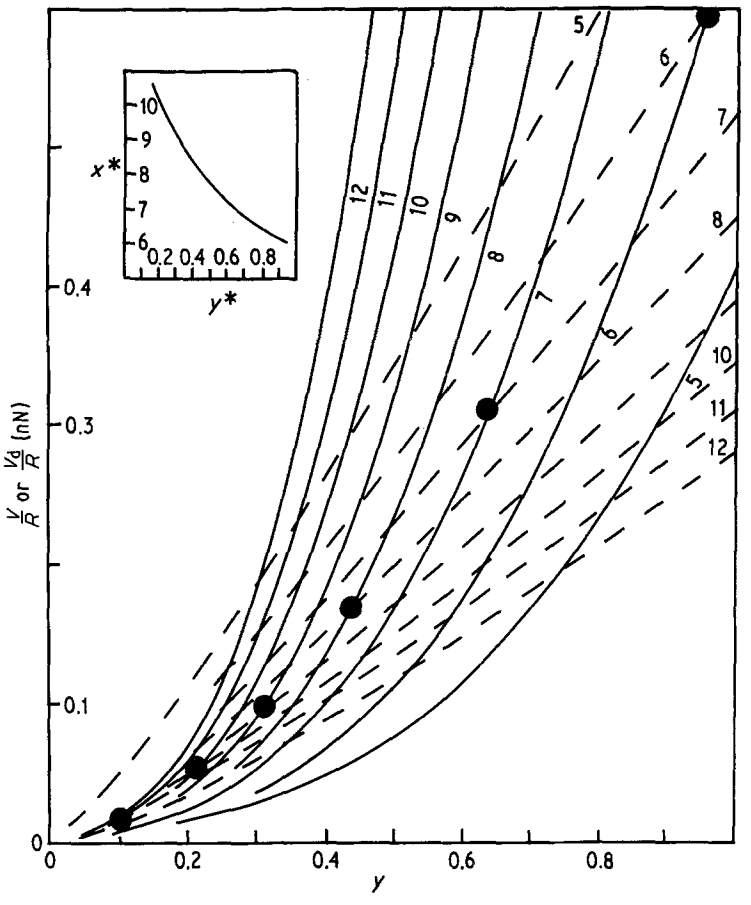

Figure 2 V/R (full lines) and V_d/R (dashed lines) against radius ratio y for Cd at 573 K, with aspect ratio x as parameter. The full circles lie on the locus of points $(V^*/R, x^*, y^*)$ for a mature raft. Inset: Aspect ratio against radius ratio for mature Cd rafts at 573 K.

expected intuitively. Intersection becomes feasible at about $x = 6$. During formation a raft spreads faster than it thickens [1]; in other words, it increases simultaneously in x and y (assuming R is constant). Its representative point on the graph of V against y will consequently move up to meet the locus of intersections $V = V_d$, and this will define a set of co-ordinates V^*, y^*, x^* which mark the attainment of maturity and the generation of a screw dislocation.

According to Fig. 2, a Cd raft of maximum radius ratio ($y^* = 0.53$) should possess an aspect ratio $7 < x^* < 8$. A more accurate reading is obtained from the inset, which gives $x^* = 7.5$. A similar value is obtained for Zn at 673 K by taking $y^* = 0.55$. When the calculations are repeated with V' instead of V the values of x^* are slightly higher.

These predictions of the aspect ratio of the mature basal raft are in harmony with rough estimates made on micrographs of solid aerosol particles [1]. The thickness of the mature raft itself cannot be measured on the solidified droplet, and estimates have had to be made on immature rafts. In addition to our evidence from aerosol particles, the sectioned Zn particle of White [16] indicates $x^* \sim 5$, although Cahn, Hillig and Sears [17] concluded that the aspect ratio of a floating raft was about 30.

The larger aerosol droplets which are condensed at background temperatures approaching the melting point were found to have y^* values of over 0.6 [2]. Other things being equal, this would suggest a correspondingly smaller x^*, and although there are no data to confirm this a lower extent of growth rate anisotropy is to be expected of particles solidifying at higher temperatures. There is, however, also a possibility of interference at these higher background temperatures by vapour growth, evaporation or surface diffusion, any of which might effect the profile of the particle after solidification and so vitiate the measurement of y^*.

Another surface feature of the solidified sphere that might afford useful data for calculations is the helix step height (HSH). This is the distance

by which the solidification front advances into the melt during one complete turn of the growth spiral, and is equal to the magnitude b of the Burgers vector of the screw dislocation or to an integral multiple of it. The fine rings observed on Cd spheres were attributed to the turns of the solidification helix [1]. A very crude estimate of the step height made by measuring the ring spacing in the micrograph of Buckle *et al.* [1] is 70 nm. Using this for b and $y^* = 0.53$ again, $x^* = 76$. Although a thinner raft must follow from a larger b the values of both b and x^* are unduly large, and in the light of the other evidence on x^* it appears that the observed HSH is not simply related to b.

For convenience of calculation the raft has been taken as elastically isotropic, so that the strained condition of the raft depends upon its aspect ratio. This, in turn, depends on the occurrence of unequal growth rates in different crystallographic directions. Anisotropy of *growth rate*, therefore, is the factor which in this theoretical treatment is vital to the onset of the helical growth mechanism. Although different growth rates may be intrinsic to the different orientations of surface planes we have neglected to take into account the possible part played by heat transfer. While it is clear that the expansion stage of raft growth is always slow relative to the eventual rate of thickening, growing rafts have been seen to move about on the drop surface [17, 18]. Such motion is suggestive of thermal gradients and the possible existence of thermal stress which play an essential role in the re-organization of the stress field and the creation of the dislocation.

Acknowledgements

We wish to thank G. J. Richardson for helpful discussions and the SRC for continued support of this programme of work.

References

1. E. R. BUCKLE, K. C. POINTON and P. TSAKIROPOULOS, *J. Mater. Sci.* **15** (1980) 2921.
2. E. R. BUCKLE and K. C. POINTON, *ibid* **12** (1977) 75.
3. W. BOAS and J. K. MACKENZIE, *Prog. Met. Phys.* **2** (1950) 90.
4. S. G. LEKHNITSKII, "Theory of Elasticity of an Anisotropic Elastic Body", translated by P. Fern (Holden-Day, San Francisco, 1963) p. 367.
5. S. P. TIMOSHENKO and J. N. GOODIER, "Theory of Elasticity", 3rd edition (McGraw-Hill, Kogakusha, Tokyo, 1970) p. 385.
6. *Idem, ibid.* pp. 15, 274.
7. *Idem, ibid.* p. 247.
8. C. J. SMITHELLS, "Metals Reference Book", Vol. 1 (Butterworths, London, 1967).
9. G. V. SAMSONOV, "Handbook of the Physico-Chemical Properties of the Elements" (Oldbourne, London, 1968).
10. D. W. G. WHITE, *Trans. Met. Soc. AIME* **236** (1966) 796.
11. *Idem, Metall. Trans.* **3** (1972) 1933.
12. J. D. ESHELBY and A. N. STROH, *Phil. Mag.* **42** (1951) 335.
13. J. D. ESHELBY, private discussion.
14. D. HULL, "Introduction to Dislocations" (Pergamon, Oxford, 1969).
15. Metals Handbook, Vol. 1 (American Society for Testing Metals, Ohio, 1961).
16. D. W. G. WHITE, *J. Inst. Met.* **99** (1971) 287.
17. J. D. CAHN, W. B. HILLIG and G. W. SEARS, *Acta Met.* **12** (1964) 1421.
18. B. MUTAFTSCHIEV and J. ZELL, *Surface Sci.* **12** (1968) 317.

Received 13 October and accepted 14 November 1980.